Adaptive Ankle Torque Control for Bipedal Humanoid Walking on Surfaces with Unknown Horizontal and Vertical Motion

Jacob Stewart*[1], I-Chia Chang*[2], Yan Gu†[2], and Petros A. Ioannou[1]

***Abstract*— Achieving stable bipedal walking on surfaces with unknown motion remains a challenging control problem due to the hybrid, time-varying, partially unknown dynamics of the robot and the difficulty of accurate state and surface motion estimation. Surface motion imposes uncertainty on both system parameters and non-homogeneous disturbance in the walking robot dynamics. In this paper, we design an adaptive ankle torque controller to simultaneously address these two uncertainties and propose a step-length planner to minimize the required control torque. Typically, an adaptive controller is used for a continuous system. To apply adaptive control on a hybrid system such as a walking robot, an intermediate command profile is introduced to ensure a continuous error system. Simulations on a planar bipedal robot, along with comparisons against a baseline controller, demonstrate that the proposed approach effectively ensures stable walking and accurate tracking under unknown, time-varying disturbances.**

I. INTRODUCTION

Bipedal robots have shown their ability to walk stably on stationary surfaces using model-based [1] or data-driven [2] methods. However, locomotion control on moving surfaces remains challenging due to the difficulty of state estimation [3], [4] and the fact that the surface motion induces unknown, time-varying disturbance in the nonlinear and hybrid dynamics of a walking robot [5], [6]. In terms of controller design, the surface motion can be treated as a known disturbance input [5] or an unknown external disturbance [7]. It can also be assumed to have either bounded acceleration in the vertical [8] or horizontal directions [9]. Previous work addressing vertical ground motions either assumes an accurately known surface movement profile [10] or ignores the horizontal ground motions [8]. Meanwhile, existing control approaches for horizontal ground movements [5] assume the surface exhibits an exactly periodic, accurately known motion [9]. Currently, controllers that explicitly treat both unknown vertical and horizontal surface motions are missing.

Adaptive control has been used in a variety of industrial applications to reject disturbances with unknown parameters affecting systems with either known or unknown dynamics. In the case of a bipedal robot walking on a moving platform such as a ship, there is often very limited knowledge of the surface movement beyond it is a sum of sinusoidal components with time-varying parameters [11], [12]. Though some adaptive control schemes can reject disturbances with minimal knowledge of the system dynamics [13], adaptive controllers that use the available knowledge of the system dynamics typically perform more effectively and have a lower computation complexity [14]. These methods are robust to measurement noise and model uncertainty [15] and can be tuned to be effective in the presence of time variations of the system parameter and disturbance frequency [16], [17]. However, adaptive controllers are typically suitable for continuous systems, and thus may not be directly applicable to walking robots, whose dynamics are inherently hybrid [1] due to the robot's feet making and breaking contact with the ground. Although adaptive control has recently been extended to hybrid systems including walking robots [18], the approach focuses on time-invariant robot dynamics rather than time-varying disturbance.

This paper introduces an adaptive ankle torque control approach that achieves stable bipedal walking during unknown horizontal and vertical ground motions. The main contributions of this study are:

(a) Introduction of a commanded state based on the modification of the desired robot state, which, despite the hybrid nature of walking robot dynamics, renders a continuous error system, allowing the direct application of existing adaptive controllers typically designed for continuous systems. This method expands the range of applications of adaptive control.
(b) Construction of an adaptive ankle torque controller that explicitly treats unknown horizontal and vertical ground motions. This controller ensures walking stability and enables accurate position tracking within continuous phases of walking. Such a performance is not achievable with previous footstep control[5], [8].
(c) Simulation validation on a seven-link biped during various surface motion.

II. PROBLEM FORMULATION

This paper focuses on designing an adaptive control approach that ensures stable bipedal walking during unknown ground motions in both horizontal and vertical directions.

To address the hybrid nature of walking, we explicitly consider the discrete events of foot touchdowns. The foot touchdown times are denoted t_k indexed by $k \in \mathbb{N}$. The instants immediately before and after touchdown are denoted

*These authors contributed equally. †Corresponding author. This material is based upon work supported by the National Science Foundation under Grants CMMI-1934280 and CMMI-2046562 and by the Office of Naval Research under Grant N00014-24-1-2028. Any opinions, findings and conclusions or recommendations expressed in this material are those of the author(s) and do not necessarily reflect the views of the National Science Foundation.

[1]Jacob Stewart and Petros A. Ioannou are with the Viterbi School of Engineering, University of Southern California, Los Angeles, CA 90007. {jacobmst, ioannou}@usc.edu.

[2]I-Chia Chang and Yan Gu are with the School of Mechanical Engineering, Purdue University, West Lafayette, IN 47907, USA. E-mails: {chang970, yangu}@purdue.edu.

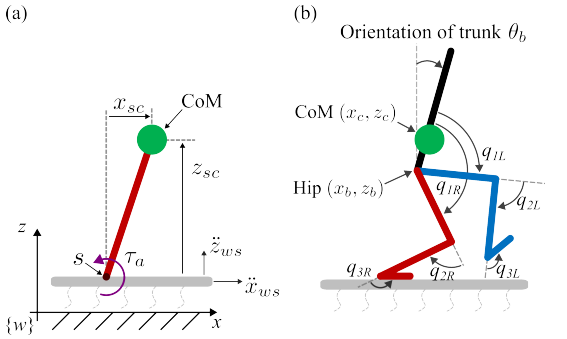

Fig. 1. (a) A linear inverted pendulum model on a platform moving along the x and z axes of the world frame $\{w\}$. (b) A seven-link robot whose state is $\mathbf{q} = [\mathbf{x}_{base}^T, \mathbf{q}_j^T]^T$, with $\mathbf{x}_{base} = [x_b, z_b, \theta_b]^T$ and $\mathbf{q}_j = [q_{1L}, q_{2L}, q_{3L}, q_{1R}, q_{2R}, q_{3R}]^T$. The variables x_b, z_b, θ_b, and the elements of $\mathbf{q}_j$ are defined as illustrated in subplot (b).

t_k^- and t_k^+, respectively. Without loss of generality and by assuming an accurate swing-foot position controller, the touchdown times are selected as $t_k = (k-0.5)T_s$, where T_s is the user-specified step period.

Based on the assumption that the mass of the robot is concentrated at the center of mass (CoM) and the angular momentum about CoM remains constant [8], we model the CoM dynamics using the disturbed variable-length inverted pendulum, as shown in Fig.1(a).

As illustrated in the Fig.1(a), $x_{sc}(t)$ and $z_{sc}(t)$ are the known horizontal and vertical position of the CoM with respect to the support point s that is fixed to the moving surface. Without loss of generality, suppose that for the actual robot shown in Fig.1(b), the vertical position $z_{sc}(t)$ is regulated (e.g., by a whole-body controller [5], [1]) to be within some bounded value z_b of the desired constant vertical position z_{sc}^d for all time; i.e., $|z_{sc}(t) - z_{sc}^d| < z_b < z_{sc}^d$ for all $t > 0$.

Using $\mathbf{x}(t) := [x_{sc}(t), \dot{x}_{sc}(t)]^T$ to denote the state of the horizontal CoM dynamics, and applying Lagrange's method, we obtain the disturbed variable-length inverted pendulum model as

$$\begin{aligned} \dot{\mathbf{x}}(t) &= \begin{bmatrix} 0 & 1 \\ \frac{g+\ddot{z}_{ws}(t)}{z_{sc}(t)} & 0 \end{bmatrix} \mathbf{x}(t) + \mathbf{B}_2 f\left(t, \mathbf{x}(t), \tau_a(t)\right), \quad t \neq t_k^- \\ \mathbf{x}(t_k^+) &= \mathbf{x}(t_k^-) - \mathbf{B}_1 u(t_k^-), \qquad\qquad\qquad\qquad t = t_k^- \end{aligned} \tag{1}$$

where $\mathbf{B}_1 = [1, 0]^T$, $\mathbf{B}_2 = [0, 1]^T$, and the function f is

$$f\left(t, \mathbf{x}(t), \tau_a(t)\right) = -\ddot{x}_{ws}(t) - \frac{\tau_a(t)}{m z_{sc}(t)}.$$

Here, m is the mass of the robot and g is the magnitude of the gravitational acceleration. $\ddot{x}_{ws}(t)$ and $\ddot{z}_{ws}(t)$ are the bounded unknown accelerations of the support point s with respect to an inertial world frame in the horizontal and vertical directions, respectively. The ankle torque $\tau_a(t)$ and the foot placement control $u(t_k^-)$ are the control signals to be designed.

This equation reveals that $\ddot{x}_{ws}(t)$ induces non-homogeneous disturbance while $\ddot{z}_{ws}(t)$ causes parametric uncertainty. Since this model considers both unknown vertical and horizontal surface motion, it is different from previous pendulum models for DRS locomotion [5] [8].

This study focuses on treating surface accelerations that are a sum of sinusoidal terms with time-varying characteristics [11], [12]; i.e., the disturbance induced by surface acceleration takes the following general form

$$\begin{aligned} \ddot{x}_{ws}(t) =& a_{x0}(t) + \sum_{i=1}^{n_x} a_{xi}(t) \sin\left(\int_0^t \omega_{xi}(\tau)\partial\tau + \varphi_{xi}\right) \\ \ddot{z}_{ws}(t) =& a_{z0}(t) + \sum_{i=1}^{n_z} a_{zi}(t) \sin\left(\int_0^t \omega_{zi}(\tau)\partial\tau + \varphi_{zi}\right) \end{aligned} \tag{2}$$

where n_x, n_z are the numbers of sinusoidal terms, $a_{x0}(t)$, $a_{z0}(t)$ are the bias terms, $a_{xi}(t)$, $a_{zi}(t)$ are the disturbance amplitudes, $\omega_{xi}(t)$, $\omega_{zi}(t)$ are the disturbance frequencies, and φ_{xi}, φ_{zi} are the disturbance phases. Assume the parameters of the disturbance are slowly varying with respect to time; i.e., there exists a parameter $\mu \geq 0$ such that $\sup_t |\square^{(k)}| \leq \mu$ for all $\square \in \{a_{xi}(t), \omega_{xi}(t), a_{zj}(t), \omega_{zj}(t)\}$, for all derivative orders $k \in \mathbb{N}$, and for all indices $i \in \{0, 1, \ldots, n_x\}$, $j \in \{0, 1, \ldots, n_z\}$. Also assume these parameters are such that the disturbances are uniformly bounded; i.e., there exists $\bar{x}, \bar{z} < \infty$ such that $\sup_t |\ddot{x}_{ws}(t)| \leq \bar{x}$ and $\sup_t |\ddot{z}_{ws}(t)| \leq \bar{z}$.

To minimize the requested ankle torque, the desired CoM motion profile is designed to be a hyperbolic profile of a linear inverted pendulum model [1] without ankle torque actuation. Specifically, the desired hyperbolic, piecewise continuous motion profile is the solution of the following hybrid system

$$\begin{aligned} \dot{\mathbf{x}}^d(t) =& \mathbf{A}_\lambda \mathbf{x}^d(t), \qquad\qquad\qquad \text{if } t \neq t_k^- \\ \mathbf{x}^d(t_k^+) =& \mathbf{x}^d(t_k^-) - \mathbf{B}_1 T_s v^d, \quad \text{if } t = t_k^- \end{aligned} \tag{3}$$

where $\mathbf{x}^d(t) =: [x_{sc}^d(t), \dot{x}_{sc}^d(t)]^T$ is the desired trajectory of $\mathbf{x}(t)$ and $\mathbf{A}_\lambda = \begin{bmatrix} 0 & 1 \\ \lambda^2 & 0 \end{bmatrix}$ with $\lambda = \sqrt{\frac{g}{z_{sc}^d}}$. To enforce the desired walking velocity v^d as the average value of $\dot{x}_{sc}^d(t)$ within each walking step, the initial condition is set to $\mathbf{x}^d(0) = [0, \frac{v^d T_s \lambda}{2\sinh(0.5\lambda T_s)}]^T$.

The control objective is to design the two control inputs, the ankle torque $\tau_a(t)$ and foot placement control $u(t_k^-)$ ($k \in \mathbb{N}$), such that (a) the ankle torque is less than a known limit $\bar{\tau}_a$ for any $t > 0$ and (b) the velocity tracking error $x_{sc}^d(t) - x_{sc}(t)$ converges to a small residual set as $t \to \infty$, in the presence of the unknown disturbances $\ddot{x}_{ws}(t)$ and $\ddot{z}_{ws}(t)$.

III. METHOD

This section presents the proposed control approach that explicitly addresses unknown vertical and horizontal ground motions to achieve stable bipedal walking.

The proposed control approach comprises three primary elements: a discrete footstep planner, a continuous stabilizing controller, and an adaptive controller. The design of the proposed approach begins with the modification of the desired hybrid trajectory of the pendulum state (3), producing a hybrid system associated with a commanded state as well as a continuous system of the actual tracking error. A discrete footstep planner is then synthesized to drive the commanded state to the desired state, while the continuous actual error

system is treated by the continuous stabilizing and adaptive controllers. The footstep planner also helps keep the required ankle torque small for the two continuous controllers.

A. Discrete Footstep Planner Based on Commanded State

To introduce a continuous error system, we construct a commanded state trajectory, $\mathbf{x}^c(t) =: \left[x^c_{sc}(t), \dot{x}^c_{sc}(t)\right]^T$, which starts at the robot's true initial state $\mathbf{x}(0)$ and converges to the desired state trajectory, $\mathbf{x}^d(t)$, as $t \to \infty$ under the proposed footstep planner. The use of $\mathbf{x}^c(t)$ aims to prevent an overly large state error when the robot starts from rest and makes the dynamics of $\mathbf{x}^c(t) - \mathbf{x}(t)$ completely continuous. This is the basis for the designs of the two proposed continuous controllers and also lowers the demand for significant control input.

To drive the commanded state $\mathbf{x}^c(t)$ toward the desired state $\mathbf{x}^d(t)$ using the foot placement control $u(t_k^-)$, we design the dynamics of $\mathbf{x}^c(t)$ as the following hybrid system

$$\begin{aligned} \dot{\mathbf{x}}^c(t) =& \mathbf{A}_\lambda \mathbf{x}^c(t), && \text{if } t \neq t_k^- \\ \mathbf{x}^c(t_k^+) =& \mathbf{x}^c(t_k^-) - \mathbf{B}_1 u(t_k^-), && \text{if } t = t_k^- \end{aligned} \tag{4}$$

To drive $\mathbf{x}^c(t)$ to $\mathbf{x}^d(t)$, we propose a linear-quadratic regulator (LQR) footstep controller, which drives the displacement traveled over one step period to $T_s v^d$ and is described by

$$u(t_{k+1}^-) = T_s v^d - \mathbf{K}(\mathbf{A}_s - \mathbf{I})\mathbf{e}^c(t_k^+) \tag{5}$$

where $\mathbf{e}^c(t) := \mathbf{x}^d(t) - \mathbf{x}^c(t)$, $\mathbf{K} = (\mathbf{R} + \mathbf{B}_s^T\mathbf{P}_s\mathbf{B}_s)^{-1}\mathbf{B}_s^T\mathbf{P}_s\mathbf{A}_s$, $\mathbf{A}_s = \exp(\mathbf{A}_\lambda T_s)$, and $\mathbf{B}_s = (\mathbf{A}_s - \mathbf{I})\mathbf{B}_1$. The matrix $\mathbf{P}_s$ is the solution to the discrete-time algebraic Ricatti equation $\mathbf{P}_s = \mathbf{A}_s^T\mathbf{P}_s\mathbf{A}_s + \mathbf{Q} - \left(\mathbf{A}_s^T\mathbf{P}_s\mathbf{B}_s\right)\left(\mathbf{R} + \mathbf{B}_s^T\mathbf{P}_s\mathbf{B}_s\right)^{-1}\left(\mathbf{B}_s^T\mathbf{P}_s\mathbf{A}_s\right)$. The matrices $\mathbf{R} > 0$ and $\mathbf{Q} \geq 0$ are the LQR parameters chosen for good performance, e.g., fast convergence to desired CoM state. Then we have the following result.

Lemma 1: The foot placment control law in (5) drives $\mathbf{e}^c(t) \to 0$ and $\mathbf{x}^c(t) \to \mathbf{x}^d(t)$ as $t \to \infty$.

Proof sketch: We first obtain the step-to-step dynamics [1] of the system with the state $[e^c, \dot{e}^c]^T$ and the input $u(t_k^-)$ using (3)-(4). Then, we apply the transform $(A_s - I)$ to obtain the error in the traveled displacement over one step period, and observe that the proposed controller will stabilize the system because the system is controllable.

B. Continuous Stabilizing Controller Based on Actual State

Prior to presenting the proposed adaptive controller, we first introduce an ankle torque controller that stabilizes the dynamics of the actual pendulum state error. This actual error is defined as the discrepancy between the current actual state and the commanded state; i.e., $\mathbf{e}(t) := \left[e_{sc}(t), \dot{e}_{sc}(t)\right]^T := \mathbf{x}^c(t) - \mathbf{x}(t)$. Based on the dynamics of the actual (1) and the commanded state (4), the error system is expressed as

$$\begin{aligned} \dot{\mathbf{e}}(t) =& \begin{bmatrix} 0 & 1 \\ \frac{\ddot{z}_{ws}(t)}{z_{sc}(t)} & 0 \end{bmatrix} \mathbf{e}(t) + \mathbf{B}_2 h\left(t, e_{sc}(t), \tau_a(t)\right), && \text{if } t \neq t_k^- \\ \mathbf{e}(t_k^+) =& \mathbf{e}(t_k^-), && \text{if } t = t_k^- \end{aligned}$$

where $h(t, e_{sc}(t), \tau_a(t)) = \frac{\tau_a(t)}{m z_{sc}(t)} + \frac{g}{z_{sc}(t)} e_{sc}(t) + \left(\frac{g}{z^d_{sc}} - \frac{g}{z_{sc}(t)}\right) x^c_{sc}(t) + \ddot{x}_{ws}(t) - \frac{x^c_{sc}(t)}{z_{sc}(t)} \ddot{z}_{ws}(t)$. Note that the dynamics of the error between the actual and commanded states is a continuous system, instead of a hybrid one with state jumps. This ensures the error observed by the adaptive controller is continuous.

To stabilize the continuous error dynamics, we design the ankle torque command as a combination of feed-forward and proportional-derivative (PD) feedback control terms:

$$\begin{aligned} \tau_a(t) = m z_{sc}(t) \Big[&\left(-\tfrac{g}{z_{sc}(t)} - k_p\right) e_{sc}(t) - k_d \dot{e}_{sc}(t) \\ &- \left(\tfrac{g}{z^d_{sc}} - \tfrac{g}{z_{sc}(t)}\right) x^c_{sc} + k_p v(t) \Big] \end{aligned} \tag{6}$$

where k_p and k_d are the PD gains and $v(t)$ is an input signal to be introduced in the next subsection. Then, the closed-loop error dynamics is given by

$$\dot{\mathbf{e}}(t) = \left(\mathbf{A} + \mathbf{\Delta}(t)\right)\mathbf{e}(t) + \mathbf{B}\left(v(t) - d(t)\right) \tag{7}$$

where $\mathbf{A} = \begin{bmatrix} 0 & 1 \\ -k_p & -k_d \end{bmatrix}$, $\mathbf{\Delta}(t) = \begin{bmatrix} 0 & 0 \\ \frac{\ddot{z}_{ws}(t)}{z_{sc}(t)} & 0 \end{bmatrix}$, and $\mathbf{B} = [0, k_p]^T$. The unknown input disturbance $d(t)$ is given by

$$d(t) = -\tfrac{1}{k_p}\left(\ddot{x}_{ws}(t) - \tfrac{x^c_{sc}(t)}{z_{sc}(t)} \ddot{z}_{ws}(t)\right). \tag{8}$$

The following lemma states that the proposed ankle torque control (6) with $v(t) = 0$ can be used to stabilize the continuous error system provided that the unknown disturbance $\ddot{z}_{ws}(t)$, which manifests as model uncertainty in the closed-loop system, is small enough not to destabilize the system.

Lemma 2: Assume $k_p, k_d > 0$ can be chosen such that $\sup_t \left|\frac{\ddot{z}_{ws}(t)}{z_{sc}(t)}\right| \leq \frac{\bar{z}}{z^d_{sc} - z_b} < \frac{1}{2\|\mathbf{L}\|}$, with $\mathbf{L} = \mathbf{L}^T > 0$ the solution to the Lyapunov equation $\mathbf{A}^T\mathbf{L} + \mathbf{L}\mathbf{A} = -\mathbf{I}$, where $\mathbf{I}$ is an identity matrix of a proper dimension. Then the controller (6) with $v(t) = 0$ drives $\mathbf{e}(t)$ to a residual set whose size is uniformly bounded and proportional to $\limsup_{t\to\infty} \left|\ddot{x}_{ws}(t) - \frac{x^c_{sc}(t)}{z_{sc}(t)} \ddot{z}_{ws}(t)\right| \leq \bar{x} + \frac{0.5 T_s v^d}{2\|\mathbf{L}\|} < \infty$.

Proof sketch: Fist, we use the Lyapunov function candidate $V = \mathbf{e}^T\mathbf{L}\mathbf{e}$ and the methods for semi-global and practical stabilization described in [19] to show that, when $|\mathbf{e}|$ is sufficiently large, $\dot{V} \leq -\left(1 - 2\sup_t \left|\frac{\ddot{z}_{ws}(t)}{z_{sc}(t)}\right| \|\mathbf{L}\|\right)|\mathbf{e}|^2 + 2\|\mathbf{L}\||\mathbf{e}| \sup_t \left|\ddot{x}_{ws}(t) - \frac{x^c_{sc}(t)}{z_{sc}(t)} \ddot{z}_{ws}(t)\right| < 0$.

C. Continuous Adaptive Controller

The adaptive controller generating the control input $v(t)$ is comprised of an observer, a compensator, and an adaptive parameter estimator. The objective of the adaptive controller is to reject the unknown disturbance $d(t)$ for the actual error dynamics in (7). The design of this controller is inspired by existing adaptive control [17] for continuous systems that include the actual error dynamics in (7).

1) Observer design: To build the observer, we introduce an observer state $\hat{\mathbf{e}}(t)$ whose dynamics does not directly depend on the disturbances (8), along with a time-varying variable $\zeta(t)$ representing the effect of (8) on the CoM position error $e_{sc}(t)$. Their dynamics are designed as:

$$\begin{aligned} \dot{\hat{\mathbf{e}}}(t) =& \mathbf{A}\hat{\mathbf{e}}(t) + \mathbf{B}v(t) \\ \zeta(t) =& \mathbf{C}\left(\mathbf{e}(t) - \hat{\mathbf{e}}(t)\right) \end{aligned} \tag{9}$$

where $\mathbf{C} = \begin{bmatrix}1 & 0\end{bmatrix}$. Here, the disturbance-induced term $\zeta(t)$ is parameterized as [20]:

$$\zeta(t) = \boldsymbol{\phi}^T(t)\boldsymbol{\theta}(t) + \kappa(t) \tag{10}$$

where $\boldsymbol{\phi} : \mathbb{R}^+ \to \mathbb{R}^{n_\phi}$ is a regressor vector with its dimension n_ϕ to be designed, $\boldsymbol{\theta} : \mathbb{R}^+ \to \mathbb{R}^{n_\phi}$ is the unknown parameter vector with $\theta_k(t)$ its k^{th} ($k \in \{1, 2, ..., n_\phi\}$) element, and $\kappa(t)$ is a bounded error term whose size is proportional to the parameter μ [17].

2) Compensator design: To construct $v(t)$ for ensuring a reasonable convergence rate of parameter estimation in practice, we utilize a compensator in the form of a parallel low-pass filter $\mathcal{L}[v(t)] = \sum_{k=1}^{n_\phi} \frac{\sigma^k}{(s+\sigma)^k} \mathcal{L}\left[\hat{\theta}_k(t)\zeta(t)\right](s)$ [15]. Here, $\hat{\boldsymbol{\theta}}(t)$ is the estimated value of the unknown parameter $\boldsymbol{\theta}(t)$, with $\hat{\theta}_k(t)$ its k^{th} element. The bandwidth parameter $\sigma > 0$ and the compensator order n_ϕ are design parameters, which can be tuned for good performance. n_ϕ must be more than twice the number of sinusoidal components in the disturbance (8) plus 1. The state-space form of the compensator that produces the input $v(t)$ is given by

$$\begin{aligned} \dot{\boldsymbol{\eta}}(t) =& \mathbf{F}\boldsymbol{\eta}(t) + \hat{\boldsymbol{\theta}}(t)\zeta(t) \\ v(t) =& \mathbf{H}\boldsymbol{\eta}(t) \end{aligned} \tag{11}$$

where $\boldsymbol{\eta} \in \mathbb{R}^{n_\phi}$ is the compensator state, $\mathbf{H} := \sigma\begin{bmatrix}1 & 0 & \cdots & 0\end{bmatrix}$, and $\mathbf{F} := \sigma(\mathbf{U} - \mathbf{I})$, with $\mathbf{U}$ an upper diagonal shift matrix with 1's along the first upper diagonal and zeros everywhere else.

3) Parameter estimation: To generate the regressor vector $\boldsymbol{\phi}(t)$ based on the known value of $\zeta(t)$, we utilize the following dynamical system [20]

$$\begin{aligned} \begin{bmatrix}\dot{\mathbf{X}}(t) \\ \dot{\mathbf{Y}}(t)\end{bmatrix} &= \begin{bmatrix}\mathbf{A} & \mathbf{BH} \\ \mathbf{0} & \mathbf{F}\end{bmatrix}\begin{bmatrix}\mathbf{X}(t) \\ \mathbf{Y}(t)\end{bmatrix} + \begin{bmatrix}\mathbf{0} \\ \zeta(t)\mathbf{I}\end{bmatrix} \\ \boldsymbol{\phi}^T(t) &= \begin{bmatrix}\mathbf{C} & \mathbf{0}\end{bmatrix}\begin{bmatrix}\mathbf{X}(t) \\ \mathbf{Y}(t)\end{bmatrix} \end{aligned} \tag{12}$$

where $\mathbf{X} \in \mathbb{R}^{2\times n_\phi}$ and $\mathbf{Y} \in \mathbb{R}^{n_\phi \times n_\phi}$ are matrix-valued states and $\mathbf{0}$ is a zero matrix/vector with a proper dimension.

The time variation of the unknown parameter vector $\boldsymbol{\theta}(t)$ motivates the generation of the estimates $\hat{\boldsymbol{\theta}}(t)$ using the modified recursive-least-squares adaptive law with exponential forgetting, resetting[21], and projection described by

$$\dot{\hat{\boldsymbol{\theta}}}(t) = \text{proj}\left(\boldsymbol{\psi}(t)\right) \tag{13}$$

where proj$(\cdot)$ represents a projection operator and $\boldsymbol{\psi}(t) := \alpha\mathbf{P}(t)\boldsymbol{\phi}(t)\epsilon(t)$. Here, $\mathbf{P}(t)$ is the covariance matrix, $\epsilon(t)$ is the normalized estimation error designed as $\epsilon(t) = \frac{\zeta(t) - \boldsymbol{\phi}^T(t)\hat{\boldsymbol{\theta}}(t)}{1+\boldsymbol{\phi}^T(t)\mathbf{P}(t)\boldsymbol{\phi}(t)}$, and the gain $\alpha > 0$ controls the learning rate (i.e., how fast $\hat{\boldsymbol{\theta}}$ is changed when the normalized estimation error $\epsilon(t)$ is non-zero and how fast the covariance matrix $\mathbf{P}(t)$ may go to zero in any direction).

The covariance matrix $\mathbf{P}(t)$ can be determined by solving $\dot{\mathbf{P}}(t) = -\alpha\frac{\mathbf{P}(t)\boldsymbol{\phi}(t)\boldsymbol{\phi}^T(t)\mathbf{P}(t)}{1+\boldsymbol{\phi}^T(t)\mathbf{P}(t)\boldsymbol{\phi}(t)} + \beta\mathbf{I} + \gamma\mathbf{P}(t) - \delta\mathbf{P}^2(t)$, where the parameter $\beta > 0$ ensures adaptation does not stop by preventing $\mathbf{P}(t)$ from going to zero in any direction, the forgetting factor $\gamma > 0$ helps account for the time variations of $\boldsymbol{\theta}(t)$ by controlling the rate at which past data is discounted, and the parameter $\delta > 0$ prevents $\mathbf{P}(t)$ from becoming unbounded in any direction.

This design of $\mathbf{P}(t)$ guarantees that $0 < \mu_L\mathbf{I} \leq \mathbf{P}(t) \leq \mu_U\mathbf{I} < \infty$ for all $t > 0$, with $\mu_L = \frac{(\gamma-\alpha)+\sqrt{(\gamma-\alpha)^2+4\delta\beta}}{2\delta}$ and $\mu_U = \frac{\gamma+\sqrt{\gamma^2+4\delta\beta}}{2\delta}$, provided that the parameters are chosen such that $0 < \mu_L < \mu_U < \infty$ and the initial value satisfies $\mu_L\mathbf{I} \leq \mathbf{P}(0) \leq \mu_U\mathbf{I}$ [21].

There are typically infinitely many choices of the parameter vectors $\boldsymbol{\theta}(t)$ that satisfy (10), which implies $\boldsymbol{\phi}$ may not be persistently exciting and parameter drift may occur [20]. To ensure $\hat{\boldsymbol{\theta}}(t)$ remains bounded, the projection function proj$(\boldsymbol{\psi})$ may be implemented as

$$\text{proj}(\boldsymbol{\psi}) = \begin{cases} \boldsymbol{\psi} - \frac{\mathbf{P}(t)\hat{\boldsymbol{\theta}}(t)\hat{\boldsymbol{\theta}}^T(t)}{\hat{\boldsymbol{\theta}}^T(t)\mathbf{P}(t)\hat{\boldsymbol{\theta}}(t)}\boldsymbol{\psi} & |\hat{\boldsymbol{\theta}}(t)| = \bar{\theta} \text{ and } \hat{\boldsymbol{\theta}}^T\boldsymbol{\psi} > 0 \\ \boldsymbol{\psi} & \text{otherwise} \end{cases}$$

The constant $\bar{\theta}$ is the upper limit of $|\hat{\boldsymbol{\theta}}|$. $\bar{\theta}$ should be selected as large as feasible when prior knowledge of the disturbance frequencies is absent, ensuring that the unknown parameter vector $\boldsymbol{\theta}(t)$ remains bounded as $|\boldsymbol{\theta}(t)| < \bar{\theta}$ for all t. Then we have the following result.

Theorem 1: The inverted pendulum described by (1) with the controller described by (6) and (9)-(13) guarantees that $\hat{\boldsymbol{\theta}}(t)$, $\mathbf{P}(t)$, $\mathbf{P}^{-1}(t)$, and all signals in the closed-loop system are uniformly bounded. Furthermore, there exist $\bar{\mu} > 0$ and $\bar{\varepsilon} \geq 0$ such that for all $\mu < \bar{\mu}$ we have $\limsup_{T\to\infty} \frac{1}{T}\int_t^{t+T} |x_{sc}^d(\tau) - x_{sc}(\tau)|^2 \partial\tau \leq \rho_0\mu + \rho_1\bar{\varepsilon}$ for some $\rho_0, \rho_1 \geq 0$.

Proof sketch: The system (7), with the control input $v(t)$, the measured output $e(t)$, and the disturbance (8), can be formulated as a special case of the sinusoidal disturbance rejection problem by using the Fourier series of the desired profile $x^d(t)$. Then, we can show that the disturbance (8) can be modeled as a sum of sinusoidal components with time-varying parameters plus an arbitrarily small model error and a decaying term. Details can be found in [22], [23], [20], [24], [15], [16], [17].

IV. CASE STUDY

To validate the proposed control approach, we present a case study on a 2-D seven-link bipedal robot that is controlled to walk on a platform moving in both vertical and horizontal directions, as shown in Fig.1(b), using MATLAB.

The overall control framework for the actual robot employs a standard three-layer structure [1], [5], [7], [8] to deal with the complex full-order robot dynamics. The key novelty of this framework lies in the design of its high-level planner, which determines the ankle torque command and desired foot placement as introduced in Sec. III. The middle-level plans the desired task-space motion trajectories that agree with the output from the high-level planner. The low-level controller then executes the motion plan. Details of the middle and low levels are omitted since they are not the focus of this work.

A. High-Level Controller

To simulate the effects of digital control implementation on hardware, we follow the methods in [21], [23] to

discretize the adaptive controller (9)-(13) with a sampling period T_{samp}. Details are omitted for space consideration. The resulting controller performs sufficiently fast for real-time implementation ($<$ 1ms).

The power spectrum of the disturbance caused by surface motion on a boat is studied in [12] and shows at most two peaks in the frequency range below 1 rad/s. To prevent the compensator from attenuating $\zeta(t)$, which results in slow learning and noise amplification [13], we select the bandwidth parameter $\sigma \gg 1$ rad/s, the PD gains k_p, k_d such that the system (7) has a bandwidth larger than 1 rad/s, and a compensator order larger than twice the number of frequencies in the disturbance plus 1 (i.e. $n_\phi \gg 5$). Guidelines for tuning the parameters α, β, γ, and δ are discussed in [21]. Specifically, we select $k_p = 25$, $k_d = 10$, $T_{samp} = 1/500$ s, $\sigma = 10$ rad/s, $n_\phi = 20$, and $\mathbf{P}(0) = 10^4\mathbf{I}$. The discrete counterparts of α, β, γ, δ, and $\bar{\theta}$ are chosen as 6×10^{-1}, 10^{-3}, 10^{-5}, 10^{-6}, 10^2, respectively.

B. Validation Results

This subsection presents the simulation results of a seven-link robot walking on a moving platform. To show the performance improvement of the proposed adaptive controller, we compare the proposed approach with (a) the hybrid time-varying linear inverted pendulum (HT-LIP) stepping controller [8] and (b) PD plus feed-forward control (PD+FF), as given in (6) with $v(t) = 0$.

Three surface motion profiles, corresponding to three cases, are utilized for performance evaluation, as summarized in Table I. Case 1 is used to establish a performance baseline in the absence of disturbances. The purpose of Case 2 is to assess the controllers' effectiveness in the presence of periodic disturbances with frequency values in the ranges discussed in [12] (i.e. less than 1 rad/s). Case 3 allows evaluation under disturbances with time-varying parameters. In all cases, the desired walking velocity is $v^d = 0.2$ m/s, the step period is $T_s = 0.5$ s, the desired CoM height is $z_{sc}^d = 0.74$ m, and the ankle torque limit is $\bar{\tau}_a = 40$ Nm.

TABLE I

MOTION PROFILE OF DYNAMIC GROUND

Case	$x_{ws}(t)$ (m)	$z_{ws}(t)$ (m)
1	0	0
2	$0.2(1-\cos(0.7t))$	$0.5(1-\cos(0.4t))$
3	$0.004t^2\sin(4t)e^{-t/5}$	$0.04(0.5\cos(6t)+\cos(0.1t^2)-1.5)$

To quantitatively evaluate the performance of the controllers, For quantitative evaluation, we generate $N = 7501$ data samples at the sample times $t_i = \frac{i-1}{500}$ s indexed by $i \in \{1, \ldots, N\}$, and define the evaluation interval as $E = \{t \mid 5s \leq t \leq 15s\}$. The evaluation interval is chosen to start at $t = 5$ s so that the controller transients have disappeared. The following metrics are calculated and used:

1) RMSE $= \sum_{t_i \in E} \sqrt{\frac{1}{M}|e_{sc}(t_i)|^2}$, where M is the number of time samples t_i in the evaluation interval E.
2) PEAK $= \max_{t_i \in E} |e_{sc}(t_i)|$.
3) TRQ $= \max_{i \in \{1,\ldots,N\}} |\tau_a(t_i)|$. Note that TRQ is not applicable (NA) for the HT-LIP controller since HT-LIP does not employ ankle torque.
4) FIT is the slope of the linear fit to $x_{s_0c}(t_i)$ for $t_i \in E$, where $x_{s_0c}(t)$ is the current horizontal position of CoM relative to the initial supporting point s_0.

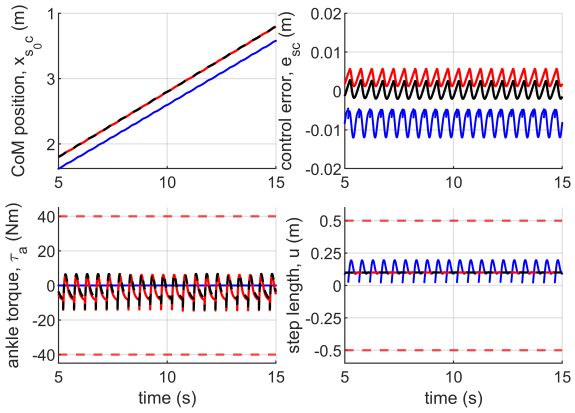

Fig. 2. Performance of the HT-LIP (blue), PD+FF (red), and proposed (black) controllers in the absence of disturbances under Case 1.

RMSE and PEAK describe the performance of the controllers over entire walking cycles. The robot's ankle motors will not be able to deliver the demanded ankle torque if TRQ exceeds the ankle torque limit $\bar{\tau}_a$, and the robot achieves the desired average walking speed when the slope of the linear fit (FIT) equals the commanded velocity v^d.

TABLE II

CONTROLLER PERFORMANCE COMPARISON

Case	Controller	RMSE	PEAK	TRQ	FIT
1	HT-LIP	8.19e-03	1.20e-02	NA	1.96e-01
	PD+FF	3.52e-03	5.67e-03	1.46e+01	**2.00e-01**
	proposed	**1.51e-03**	**2.79e-03**	**1.39e+01**	**2.00e-01**
2	HT-LIP	1.43e-02	4.00e-02	NA	1.75e-01
	PD+FF	4.08e-03	9.08e-03	1.82e+01	**2.00e-01**
	proposed	**1.75e-03**	**4.17e-03**	**1.65e+01**	**2.00e-01**
3	HT-LIP	4.39e-02	1.08e-01	NA	1.70e-01
	PD+FF	1.38e-02	2.38e-02	4.33e+01	**2.00e-01**
	proposed	**3.09e-03**	**7.84e-03**	**3.43e+01**	1.99e-01

Table II summarizes the scores for the different combinations of controllers and cases. Note that the parameters of the baseline approaches are tuned for their best performance. Figure 2 shows the performance for Case 1. Figure 2 and Table II confirm that all controllers stabilizes the robot and achieves an average velocity close to the desired velocity. The actuation provided by the ankle motor improves performance over the HT-LIP controller, and the adaptive controller further enhances the performance by compensating for the bias left behind by the PD+FF controller. The bottom two plots in Figure 2 display how the different controllers adjust the control inputs to achieve the control objective.

Figure 3 presents the results for Case 2. The disturbance produces a periodic signature in Figure 3. The adaptive controller performs the best while the HT-LIP controller performs the worst, according to the metrics in Table II.

Figure 4 illustrates the performance for Case 3. The upper left plot of Figure 4 and Table II indicate that the HT-

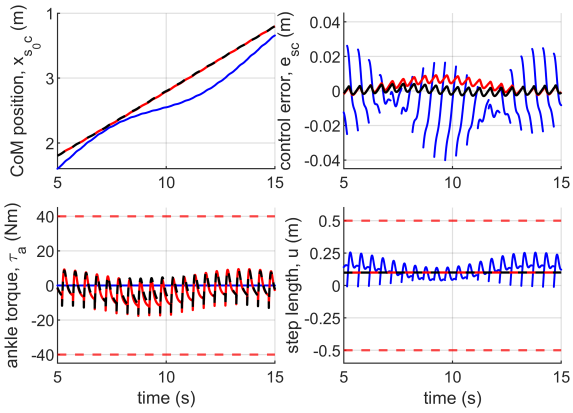

Fig. 3. Performance of the HT-LIP (blue), PD+FF (red), and proposed (black) controllers for small amplitude disturbances under Case 2.

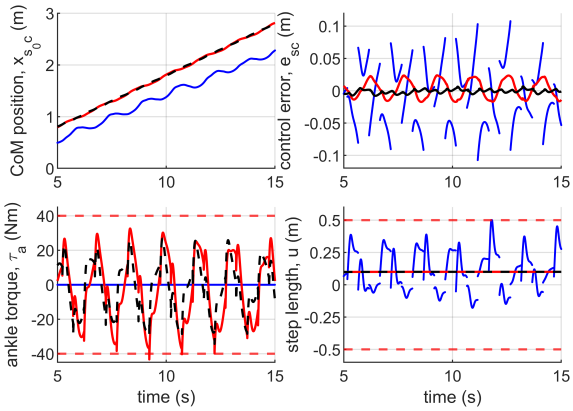

Fig. 4. Performance of the HT-LIP (blue), PD+FF (red), and proposed (black) controllers for time-varying disturbances under Case 3.

LIP controller is unable to achieve the desired velocity. The bottom left plot of Figure 4 shows the PD+FF controller exceeds the ankle torque limit just prior to 10 s. In contrast, the metrics in Table II confirm that the proposed controller not only respects the torque limit but also accurately tracks the desired position and velocity.

V. CONCLUSIONS

This paper has presented an adaptive control scheme to enable a bipedal robot to walk stably on a surface with unknown vertical and horizontal motions. By modifying the desired state trajectory, the hybrid error dynamics of the walking robot was first transformed into a continuous system, facilitating the use of adaptive control typically suited for continuous systems. Adaptive ankle torque control was then formed to reject the unknown disturbances. Simulations on a seven-link biped demonstrated the superior capability of the proposed approach in achieving accurate position and respecting joint torque limits, compared to baseline methods. Future work will focus on extending this control scheme with a feedback law to adjust the actual foot placement online and conducting experimental validations on hardware.

REFERENCES

[1] X. Xiong and A. Ames, "3-d underactuated bipedal walking via h-lip based gait synthesis and stepping stabilization," *IEEE Trans. Rob.*, vol. 38, no. 4, pp. 2405–2425, 2022.

[2] M. Dai, X. Xiong, J. Lee, and A. D. Ames, "Data-driven adaptation for robust bipedal locomotion with step-to-step dynamics," in *Proc. IEEE Int. Conf. Intel. Rob. Syst.*, 2023, pp. 8574–8581.

[3] Z. He, S. Teng, T.-Y. Lin, M. Ghaffari, and Y. Gu, "Legged robot state estimation within non-inertial environments," *arXiv preprint arXiv:2403.16252*, 2024.

[4] Y. Gao, C. Yuan, and Y. Gu, "Invariant filtering for legged humanoid locomotion on a dynamic rigid surface," *IEEE/ASME Trans. Mechatron.*, vol. 27, no. 4, pp. 1900–1909, 2022.

[5] Y. Gao, Y. Gong, V. Paredes, A. Hereid, and Y. Gu, "Time-varying alip model and robust foot-placement control for underactuated bipedal robotic walking on a swaying rigid surface," in *Proc. Amer. Contr. Conf.*, 2023, pp. 3282–3287.

[6] A. Iqbal, Y. Gao, and Y. Gu, "Provably stabilizing controllers for quadrupedal robot locomotion on dynamic rigid platforms," *IEEE/ASME Trans. Mechatron.*, vol. 25, no. 4, pp. 2035–2044, 2020.

[7] Z. Gu, R. Guo, W. Yates, Y. Chen, Y. Zhao, and Y. Zhao, "Walking-by-logic: Signal temporal logic-guided model predictive control for bipedal locomotion resilient to external perturbations," in *Proc. IEEE Int. Conf. Rob. Autom.*, 2024, pp. 1121–1127.

[8] A. Iqbal, S. Veer, and Y. Gu, "Asymptotic stabilization of aperiodic trajectories of a hybrid-linear inverted pendulum walking on a vertically moving surface," in *Proc. Amer. Contr. Conf.*, 2023, pp. 3030–3035.

[9] K. Chen, X. Huang, X. Chen, and J. Yi, "Contingency model predictive control for bipedal locomotion on moving surfaces with a linear inverted pendulum model," *arXiv preprint arXiv:2404.12455*, 2024.

[10] A. Iqbal, S. Veer, and Y. Gu, "Analytical solution to a time-varying lip model for quadrupedal walking on a vertically oscillating surface," *Mechatron.*, vol. 96, p. 103073, 2023.

[11] P. Han, G. Li, S. Skjong, B. Wu, and H. Zhang, "Data-driven sea state estimation for vessels using multi-domain features from motion responses," in *Proc. IEEE Int. Conf. Rob. Autom.*, 2021, pp. 2120–2126.

[12] E. A. Tannuri, J. V. Sparano, A. N. Simos, and J. J. Da Cruz, "Estimating directional wave spectrum based on stationary ship motion measurements," *Appl. Oc. Res.*, vol. 25, no. 5, pp. 243–261, 2003.

[13] S. Jafari and P. A. Ioannou, "Overparameterized robust mrac for rejection of unknown periodic disturbances acting on unknown plants in the presence of noise," in *MED*, 2017, pp. 822–827.

[14] I. D. Landau, A. C. Silva, T.-B. Airimitoaie, G. Buche, and M. Noe, "Benchmark on adaptive regulation—rejection of unknown/time-varying multiple narrow band disturbances," *Eur. J. Control*, vol. 19, no. 4, pp. 237–252, 2013.

[15] S. Jafari and P. A. Ioannou, "Rejection of unknown periodic disturbances for continuous-time mimo systems with dynamic uncertainties," *Int. J. Adapt. Control Signal Process*, vol. 30, no. 12, pp. 1674–1688, 2016.

[16] J. Stewart and P. Ioannou, "Rejection of sinusoidal disturbances with unknown slowly time-varying frequencies for linear time-invariant systems," *IEEE Trans. Autom. Contr.*, vol. 69, no. 8, pp. 5531–5537, 2024.

[17] J. Stewart and P. A. Ioannou, "Rejection of Sinusoidal Disturbances With Unknown Slowly Time-Varying Frequencies for Linear Time-Varying Systems," *J. Dyn. Sys., Meas., Control.*, vol. 146, no. 4, p. 041003, 03 2024. [Online]. Available: https://doi.org/10.1115/1.4064748

[18] Y. Gu and C. Yuan, "Adaptive robust tracking control for hybrid models of three-dimensional bipedal robotic walking under uncertainties," *J. Dyn. Sys., Meas., Control.*, vol. 143, no. 8, p. 081007, 2021.

[19] A. Isidori, *Lectures in feedback design for multivariable systems*. Springer, 2017.

[20] P. A. Ioannou and J. Sun, *Robust adaptive control*. PTR Prentice-Hall Upper Saddle River, NJ, 1996, vol. 1.

[21] M. Salgado, G. Goodwin, and R. Middleton, "Modified least squares algorithm incorporating exponential resetting and forgetting," *Int. J. Control*, vol. 47, no. 2, pp. 477–491, 1988.

[22] K. S. Tsakalis and P. A. Ioannou, *Linear time-varying systems: control and adaptation*. USA: Prentice-Hall, Inc., 1993.

[23] P. Ioannou and B. Fidan, *Adaptive Control Tutorial*. Philadelphia, PA: Society for Industrial and Applied Mathematics, 2006.

[24] S. Jafari, P. Ioannou, B. Fitzpatrick, and Y. Wang, "Robustness and performance of adaptive suppression of unknown periodic disturbances," *IEEE Trans. Autom. Control.*, vol. 60, no. 8, pp. 2166–2171, 2015.